Title
Injection of Microporous Annealing Particle (MAP) Hydrogels in the Stroke Cavity Reduces Gliosis and Inflammation and Promotes NPC Migration to the Lesion

Authors
Nih, Lina R
Sideris, Elias
Carmichael, S Thomas
et al.

Peer reviewed

Brain Transplantation of Microporous Particle Hydrogel After Stroke Promotes Tissue Repair and Endogenous NPC Recruitment to the Lesion

Lina R. Nih[1,2,*], **Elias Sideris**[1,*], **S. Thomas Carmichael**[2], and **Tatiana Segura**[1,**]

[1]Department of Chemical and Biomolecular Engineering, University of California, Los Angeles, 420 Westwood Plaza, CA 90095, USA

[2]Department of Neurology, David Geffen School of Medicine, University of California, Los Angeles, 621 Charles Young Drive, CA 90095, USA

Abstract

With the number of deaths due to stroke decreasing, more individuals are forced to live with crippling disability resulting from the stroke. To date, no therapeutics exist after the first 4.5 hours after the stroke onset, aside from rest and physical therapy. Following stroke, a large influx of astrocytes and microglia releasing pro-inflammatory cytokines leads to dramatic inflammation and glial scar formation, affecting brain tissue's ability to repair itself. Pathological conditions such as a stroke trigger neural progenitor cells (NPCs) proliferation and migration toward the damaged site. However, these progenitors are often found far from the cavity or the peri-infarct tissue. Post stroke tissue remodeling results in a compartmentalized cavity that can directly accept a therapeutic material injection. Here, we show that the injection of a porous hyaluronic acid hydrogel into the stroke cavity significantly reduces the inflammatory response following stroke while increasing peri-infarct vascularization compared to non-porous hydrogel controls and stroke only controls. In addition, we show that the injection of our material impacts NPCs proliferation and migration at the subventricular zone niche and results, for the first time, in NPC migration into the stroke site.

Graphical abstract

Particle hydrogels can be injected into the stroke cavity and anneal *in situ* to form a microporous scaffold in a minimally invasive procedure. We show that this particle hydrogel scaffold decreases gliosis, while increasing the peri-infarct vasculature and promoting neural progenitor cell infiltration into the hydrogel.
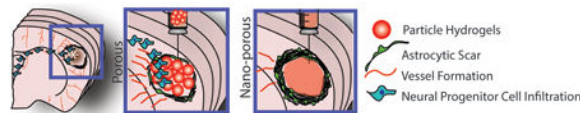
[**]Corresponding author: Prof. Tatiana Segura, Tel.: +1-310-206-3980, tsegura@ucla.edu.
[*]These authors contributed equally to this work

Keywords

Particle Hydrogels; Porous Hydrogels; Stroke; Neural Progenitor Cells; Inflammation

---

Stroke is the leading cause of long-term disability worldwide [1]. Ischemic stroke occurs when there is a decrease in cerebral blood flow due to an embolus or local thrombosis causing brain tissue damage and loss of function[2]. To date, intravenous thrombolysis and reperfusion therapies using intravenously administered recombinant tissue plasminogen activator (tPA) are the only effective therapies to treat stroke[3]. However, tPA is only effective during the first 4.5 hours after stroke onset, resulting in only about 5% of stroke patients benefiting from this treatment and leaving the majority of patients with long term disability[2, 4]. Besides physical therapy, there are no FDA approved therapies that promote recovery from the long-term disability caused by stroke, leaving an increasing number of patients with limited options[5]. Over the past few years, new strategies aimed at enhancing post-stroke brain plasticity have utilized trophic factors, stem cell therapies or combinations of the two in an effort to decrease the disability burden[6]. One goal in these therapies is to promote neural progenitor cell (NPC) migration towards the stroke site in efforts to promote neurogenesis in and around the lesion. NPCs hold great promise for stroke repair because of their potential to generate all neural cell types present in the brain[7]. The stroke alone causes a substantial increase in NPC proliferation in the SVZ[8]; however, these NPCs do not reach the stroke site itself in large numbers if it is distant to the SVZ[9]. Thus, approaches to further guide NPC migration towards the stroke site do so by delivering exogenous growth factors and cytokines to stimulate migration towards the stroke site, and differentiation into neurons[10]. Although improved NPC numbers in the peri-infarct area are observed, these NPCs are do not localize within the close damage to the stroke or into the stroke cavity[9]. Herein, we present a material that for the first time promotes the infiltration of endogenous NPCs from the SVZ into the stroke cavity.

Stroke offers a unique opportunity for a tissue engineering neural repair therapy. After initial cell death in stroke, the clearance of debris in the lesion leaves a compartmentalized cavity that can accept a large volume transplant without further damaging the surrounding healthy parenchyma [11, 12]. This stroke cavity is situated directly adjacent to the peri-infarct tissue, the region of the brain that undergoes the most substantial repair and recovery, meaning that any therapeutic delivered to the cavity will have direct access to the tissue target for repair[13]. Our laboratory and others have investigated the use of injectable hydrogels injected post stroke to promote brain repair. These hydrogels are delivered to the mentioned stroke cavity, to the peri-infarct area or to the brain surface loaded with cells, trophic factors and/or growth factors[14]. Hyaluronic acid (HA) is an ideal choice to generate materials for brain repair. HA, unlike collagen, is abundantly found in the brain, particularly in the endogenous environment for neural progenitor cells (NPCs) [15] and is both a biocompatible and bioresorbable material[16]. We have previously reported the use of nonporous hyaluronic acid hydrogels crosslinked in situ via thiol/acrylamide Michael type addition for brain repair[6, 17, 18]. These materials demonstrated biocompatibility after transplantation *in vivo* when degradable soft materials were used, and the ability to promote vascular infiltration within the stroke cavity through delivery of vascular endothelial growth factor [18] or cells

into the stroke cavity[6, 17]. However, these approaches did not result in enhanced endogenous NPC migration to the stroke cavity. Similar approaches using hyaluronic acid hydrogels that sustain delivery of a direct neurogenesis-inducing growth factors, such as brain-derived neurotrophic factor, do not induce neuroblast migration into the stroke cavity[12].

Here, we demonstrate that injectableparticle hydrogels—termed "Microporous Annealed Particle" or MAP hydrogels—induce a tissue response that unlike nonporous materials leads to progenitor cell migration into the stroke cavity. In this material, hydrogel microspheres are annealed to each other to form a bulk scaffold and pore size is determined by the random packing of the microspheres. Like their non-porous counterpart, this MAP hydrogel has the benefit of being entirely injectable, which allows for a seamless boundary in addition to microporosity. Our particle hydrogel is injected as a μgel particle slurry directly to the stroke cavity, anneals in situ, and forms an interconnected porous scaffold that fills the entire cavity. This porous scaffold interacts with cells through integrin adhesion peptides and mediates rapid cellular infiltration through microporosity of the scaffold without the need for bulk scaffold degradation. Previously poly(ethylene glycol) based particle hydrogels where shown to form mechanically stable scaffolds that enhanced cutaneous healing *in vivo*[19]. Here, HA MAP gels reduce brain inflammation post stroke, by promoting astrocyte infiltration into the stroke cavity rather than scar formation and reducing the total number of reactive microglia within the infarct. These events lead to an environment that allows neuroprogenitor cell migration into the material and stroke cavity.

HA MAP hydrogels were synthesized in three stages as previously described[20]. First, hyaluronic acid was modified through carbodiimide chemistry to introduce crosslinkable acrylamide groups (HA-Ac) on the HA backbone. Second, this polymer was modified with three peptides (adhesion peptide RGD and two Factor XIIIa substrates: Ac-FKGGERCG-NH_2, K-peptide and Ac-NQEQVSPLGGERCG-NH_2, Q-peptide), and then crosslinked through Michael-type addition using a dicysteine-containing matrix metalloproteinase degradable peptide. The crosslinking takes place in an oil-coated aqueous droplet generated in a microfluidic device, resulting in highly monodisperse beads, or microgels (μgels), that will serve as MAP-gel building blocks (Scheme. 1). These μgels were purified to remove oil and surfactants using repeated washing with buffer and centrifugation. Third, the μgels were linked to each other with factor XIIIa to form an annealed solid with void spaces (S. Figure 1). The MAP hydrogel was labeled during μgel generation (step two described above) using a malemide-containing fluorophore such that the MAP scaffold can be imaged with standard confocal microscopy after sectioning (Scheme 1A).

The droplet microfluidic device is show in (Scheme 1A). HA-Ac solution pre-reacted with the K, Q, and RGD peptides was flowed through one channel and MMP sensitive cross-linker was flowed in the second channel. These two channels merge to form the hydrogel precursor solution, which is quickly pinched by heavy mineral oil containing 1% surfactant to form μgels. The flow regime used (1 μL/min for the aqueous flow and 8 μL/min for the oil flow) produced a relatively narrow range of μgel sizes with an average μgel diameter of 45μm (Scheme 1B,C). To determine the mechanical properties of annealed scaffolds purified μgels were mixed with activated FXIII (FXIIIa) and allowed to anneal for 90 minutes.

Instron mechanical testing on the resulting annealed scaffold revealed a Young's Modulus of 1510 Pa (Scheme 1D), which closely matches the stiffness of native cortex tissue of the brain[17] Moreover, a concentrated solution of non-annealed microgels does not exhibit the mechanical properties of an annealed scaffold (S. Figure 1D). Further, through Atomic Fluorescence Microscopy (AFM) of individual microgels and instron mechanical testing of annealed scaffold we have shown that the mechanical stiffness of individual microgels closely matches the mechanical stiffness of annealed scaffolds. Finally, we have previously conducted degradation studies and have shown that the microgels degrade in the presence of collagenase I[20].

Our goal is to design HA MAP gels to promote brain tissue repair after stroke. Thus, we first studied the hydrogel injection and immune reaction toward HA MAP scaffolds to ensure that they will not further aggravate the brain damage after stroke. Brain ischemic strokes in the sensorimotor cortex were created using a middle cerebral artery occlusion (MCAo) model[21]. HA MAP or HA nanoporous (HA NP) hydrogels (6μL) were injected into the cavity five days post stroke and animals were sacrificed 10 days post injection. A group of mice with stroke but no gel injection (No Gel) was used as a negative control. MAP injection into the stroke cavity did not cause brain swelling or deformation and filled the entire cavity (Figures 1A and 2A), indicating that the gel injection and hydrogel annealing in situ did not affect the brain structure. We next analyzed the inflammatory response to hydrogels by assessing astrogliosis (Figure 1B) and microgliosis (Figure 1C) 10-days post injection. Astrogliosis was assessed through GFAP (Glial Fibrillary Acidic Protein) staining by measuring the astrocytic scar thickness and total percent positive signal in the infarct (within the stroke) and peri-infarct (around the stroke) regions. We observed a drastic decrease in the astrocytic scar thickness surrounding the MAP gel compared to the nano-porous (npore) gel and the No gel condition (No Gel) (Figure 1D). The scar in the MAP condition was only 43±8 μm thick while in the nano-porous gel and No gel conditions, the scar was 234±54 and 325±69 μm thick, respectively, almost a 6× difference. This led to a lower percentage of astrocytes in the peri-infarct area of the MAP gel condition (Figure 1C). These results show that introducing a hydrogel decreases the scar thickness, while introducing microporosity in the hydrogel drastically reduces the scar thickness. However, analysis of the GFAP signal within the stroke cavity revealed a statistical increase for both the MAP condition and the nano-porous condition compared to the No gel control (Figure 1D). This observation was surprising as we have not previously observed substantial GFAP positive cells infiltrating the stroke cavity. Further analysis showed that MAP gel injection promoted astrocyte infiltration into the infarct with an average infiltration length of 279±71 μm compared to only 42±19 μm in the nano-porous condition causing a higher percentage of astrocytes to occupy the infarct area in the MAP gel condition (Figure 1D). Interestingly these differences in astrocyte infiltration are due to the topography of the scaffold alone as the MAP and nano-porous scaffolds have the exact same biochemical signals and bulk moduli. To our knowledge this is the first time a porous hydrogel has been injected into the brain.

Similarly, significant differences in microglial response, assessed by the Iba-1 (Ionized calcium binding adaptor molecule-1) signal were observed (Figure 1E). The percent area occupied by the microglia was significantly reduced in both the infarct and peri-infarct areas

in the MAP gel condition compared to the nano-porous and No gel conditions. While only 19% of the infarct area was positive for microglia in the MAP condition, 58% of the infarct area in the nano-porous condition and 50% in the No gel conditions were positive for Iba-1. Again the differences observed are solely due to the porosity of the gel and further support previous findings that the transplantation of porous materials in other tissues lead to a decrease in inflammatory cells in and around the scaffold implant site[19, 22]. Taken together we show that both astrogliosis and microgliosis are significantly reduced in animals injected with MAP gels resulting in reduced scar thickness and decreased reactive microglia.

Once we had examined the inflammatory response, we observed cells within the infarct of the MAP condition that were not stained for astrocytes or microglia. Therefore, we wanted to determine the phenotype of those cells by investigating the vascular (S. Figure 2A) and axonal infiltration (S. Figure 2B) in both conditions. Based on our experience with MAP gels in skin[19] we expected to observe significant vascular ingrowth into the MAP scaffold but not in the nano-porous scaffold. However, we found very little vascular infiltration into the stroke/hydrogel region in all three conditions. Further analysis showed a significantly higher percentage of vessels in the peri-infarct area of the MAP gel (22%) compared to both nano-porous gel and No gel conditions (6%) (S. Figure 2B). These results highlight the fact that different tissues have substantially different post-implantation reactions to the same material. Brain tissue remodels slower than skin tissue and will likely require other bioactive signals beyond the scaffold for revascularization such as growth factors. The increase of vessels in the peri-infarct area for MAP over nano-porous is interesting because the material has no contact with this area. This implies that the inflammatory reaction in the MAP-treated animals lead to a pro-angiogenic peri-infarct environment. To assess axonal infiltration, we stained for the axonal marker NF200, which stains for the neurofilament cytoskeleton of axons and quantified the positive signal within the infarct area. We observed no differences in axonal processes into the stroke site (S. Figure 2D).

Progenitor cell migration towards the damaged tissue is a post-stroke spontaneous endogenous response to promote tissue repair. However, due to inhibitory environmental cues at the injury site these progenitor cells do not always reach the diseased tissue nor lead to tissue repair[9]. In the brain, neural progenitor cells (NPCs) reside in the subventricular zone (SVZ) and the dentate gyrus (DG) and are activated after injury to proliferate, migrate and differentiate toward the injured tissue[23]. Thus, we next investigated NPC activation and whether our material increased their proliferation and migration from the SVZ (Figure 2). To identify the NPCs we stained for double cortin (DCX) and for proliferating cells using Ki67. Cells that are double positive for DCX and Ki67 are considered proliferating NPCs (Figure 2A). Three separate analyses were performed to characterize NPC activation: the cell number along the ventricle wall, the migrating cell number, and the migration distance from the SVZ (Figure 2B). Upon injury the NPC population begins to divide to self-renew[8]. We found that for animals injected with MAP hydrogels there was an average of 34±6 NPCs per section along the ventricle wall, while the nano-porous treated animals had a significantly lower average of 18±3 NPCs, a number similar to the No Gel condition (Figure 2C). As expected, NPCs were observed migrating along the corpus callosum towards the infarct. Almost triple the amount of proliferating NPCs were counted migrating towards the damaged tissue in the MAP condition versus the nano-porous and No gel condition. The

analysis of the migration distance from the tip of the ventricle toward the leading edge of the migrating cells revealed that the NPCs in the MAP condition migrated an average of 1mm compared to less than 0.5 mm in the nano-porous condition. No differences were observed in both the NPC cell number along the ventricle wall and the migrating cell number between the nano-porous and No Gel condition, however, in the No Gel condition, the NPCs migrated less than 0.23 mmn, less than half of the nano-porous condition (Figure 2C).

We next examined the peri-infarct and infarct areas to determine if NPCs were able to reach the infarct site at 10-days post implantation (Figure 3). To our surprise we observed NPCs not only in the peri-infarct area but also in the infarct area of the MAP hydrogel condition only (Figure 3A, B). Indeed, no NPCs migration into the stroke area was observed in both the nano-porous and the No gel conditions. This is an interesting piece of data as migrating NPCs into a damaged post-stroke site has never been observed before. The NPCs migrated as far as 300 μm into the MAP scaffold and occupied 3.75%±1.2 of the stroke surface (Figure 3C). Interestingly, the migration pattern and distance appeared to be similar to that observed for astrocytes. Co-staining for NPC and astrocytes showed that the NPCs co-localized with the infiltrating astrocytes, suggesting that astrocyte penetration is paving a path for NPC infiltration. More studies need to be performed to better understand how astrocytes are guiding NPC migration into the damaged site and whether the astrocyte and NPC infiltration happens simultaneously or in sequence.

In conclusion, we demonstrate that injectable particle hydrogels—MAP hydrogels—accelerate brain repair processes by altering post-stroke astroglyosis and inflammation, changes that lead to enhanced vascularization at the peri-infarct cavity and neural progenitor cell migration within the damaged site. The present material contains hyaluronic acid, MMP, K, Q and RGD peptides as bioactive signals. Although it is likely that during the FXIIIa enzyme mediated annealing process, endogenous proteins present in the stroke cavity are incorporated into the material via the same chemistry, we do not believe this is the reason for the observed differences in inflammatory response upon material injection because FXIIIa enzyme was also added to the HA non porous condition. Rather, we believe that the porosity of the scaffold allows for a cell infiltration into the MAP hydrogel independently of scaffold degradation. The nano-porous hydrogel contains the same bioactive components and it did not result in reduced inflammatory reaction or NPC infiltration.

Experimental Section

Microgel Production and Purification

Microfluidic devices[19] and microgels[20] were produced as previously described. Briefly, an acrylate functionalized hyaluronic acid (HA) was dissolved at 7% (w/v) in 0.3M triethyloamine (TEOA) pH 8.8 and pre-reacted with K-peptide (Ac-FKGGERCG-NH$_2$), Q-peptide (Ac-NQEQVSPLGGERCG-NH$_2$), and RGD (Ac-RGDSPGERCG-NH$_2$) at a final hydrogel concentration of 250μM, 250μM, and 500μM, respectively. Mean while, the cross-linker solution was prepared by dissolving the di-thiol matrix metalloproteinase (MMP) sensitive linker peptide (Ac-GCRDGPQGIWGQDRCG-NH$_2$, Genscript) in distilled water at 7.8 mM and reacted with 10 μM Alexa-Fluor 488-maleimide (Life-Technologies) for 5 minutes. These solutions were mixed in a flow focusing microfluidic device and then

immediately pinched by 1% span-80 in heavy mineral oil to form microspheres. These microspheres are collected and allowed to gel overnight to form microgels. The microgels are then purified by repeated washes with buffer and centrifugation. We've previously characterized the swelling ratio of microgels when purified from the oil phase to the aqueous phase and found a 3.4× volumetric increase[20].

Generation of scaffold from microgels and mechanical testing

The microgels were pelleted by centrifuging at 18,000 G and discarding the supernatant to form a concentrated solution of microgels. 5 U/mL of FXIII and 1 U/mL of Thrombin were combined in the presence of 10mM Ca^{2+} with the pelleted μgels and mixed via thorough pipetting before injection and allowed to incubate at 37 °C for 90 minutes between two slides (1mm thickness) surface coated with sigmacote (Sigma-Aldrich). The mechanical testing on the hydrogel scaffolds was done using a 5500 series Instron. After annealing, the scaffolds were allowed to swell in HEPES buffer saline for 4 hours at room temperature. A 2.5N load cell with a 3.12mm tip in diameter was used at a compression strain rate of 1mm/min and the hydrogel scaffold was indented 0.8mm or 80% of its total thickness.

Nanoporous Hydrogel Production

Nanoporous hydrogel precursor solutions were exactly the same as the microgel precursor solutions. As described in the *Microgel Production and Purification* experimental section, an acrylate functionalized hyaluronic acid (HA) was dissolved at 7% (w/v) in 0.3M triethyloamine (TEOA) pH 8.8 and pre-reacted with K-peptide (Ac-FKGGERCG-NH$_2$), Q-peptide (Ac-NQEQVSPLGGERCG-NH$_2$), and RGD (Ac-RGDSPGERCG-NH$_2$) at a final hydrogel concentration of 250μM, 250μM, and 500μM, respectively. The molar ratio of acrylates to HA was 18.32, giving a concentration of 10.39mM of total acrylates. The total concentration of peptides was 1mM, giving a molar ratio 0.0962 moles of peptides per moles of acrylate. Finally, the molar ratio of thiols from cross-linker to moles of initial acrylates was 0.8, which gave a concentration of 8.31mM of thiols from cross-linker. The molar ratio of thiols from cross-linker to acrylates available after peptide conjugation was 0.88. The HA precursor solution was mixed with the peptides and allowed to react for 30 minutes before adding the cross-linker, FXIII, and thrombin. Using the precursor solution with the same concentration of peptides as the precursor solution to the microgels ensures that the concentration of peptides in the nanoporous hydrogel is the same as in the microgels. Moreover, the same cross-linker solution was prepared by dissolving the di-thiol MMP sensitive linker peptide in distilled water at 7.8 mM and reacted with 10 μM Alexa-Fluor 647-maleimide for 5 minutes. These two solutions were thoroughly mixed in an Eppendorf tube by vortexing and pipetting. 5 U/mL of FXIII and 1 U/mL of Thrombin were added to the solution and the nanoporous hydrogel was allowed to gel *in situ* via the same Michael type addition in which the microgels were individually formed. The purpose of the addition of FXIII and thrombin was to mimic the microgel injections and to ensure that any phenomenon we observe was not because of the added enzymes. Furthermore, scanning electron microscopy (SEM) has been previously used to visualize the mesh size of these HA nanoporous hydrogels[24].

Animal stroke model and immunohistological staining

Animal procedures were performed in accordance with the US National Institutes of Health Animal Protection Guidelines and the University of California Los Angeles Chancellor's Animal Research Committee. The mouse model of stroke was performed as previously described[25]. Briefly, a permanent cortical stroke was induced by a middle cerebral artery occlusion (MCAo) on young adult C57BL/6 male mice (8-12 weeks) obtained from Jackson laboratories. Briefly, under anesthesia, a small craniotomy was made over the left parietal cortex where an anterior branch of the distal middle cerebral artery was then exposed, electrocoagulated, cut to be permanently occluded, and bilateral jugular veins were clamped for 15 min. Five days following stroke surgery, microgels with FXIIIa were loaded into a Hamilton syringe (Hamilton Reno, NV) connected to a pump and 6 μL of microgels were injected into the stroke cavity using a 30-gauge needle at stereotaxic coordinates 0.26 mm anterior/posterior (AP), 3 mm medial/lateral (ML), and 1 mm dorsal/ventral (DV) with an infusion speed of 1μL/min. The needle was withdrawn from the mouse brain 5 minutes after the injection to allow for microgel annealing. Before injection, microgels were kept on ice to ensure that very little to no annealing would take place in the syringe during injection and all the annealing would occur *in situ* since FXIIIa has its highest activity at 37°C. This was done to maintain consistency between the nanoporous and MAP conditions since it has been the shown that the mode of implantation plays a drastic role in the tissue response[26]. Preliminary observations showed that withdrawing the needle from the brain immediately after MAP gel injection was associated with a rapid and instant backflow of the gel, suggesting that the injected gel had not annealed by the end of the injection time (S Video 1). However, leaving the needle in place for 5 minutes after gel injection was not associated with any backflow, suggesting that the injected gel had begun annealing and forming a scaffold in the stroke cavity. For the nanoporous condition, 6 μL of hydrogel precursor solution (HA-Acrylate + Peptides + MMP sensitive cross-linker) with FXIIIa were injected into the stroke cavity using a 30-gauge needle at stereotaxic coordinates 0.26 mm anterior/posterior (AP), 3 mm medial/lateral (ML), and 1 mm dorsal/ventral (DV) with an infusion speed of 1μL/min. Ten days following the hydrogel transplantation, mice were sacrificed via transcardial perfusion of 0.1 M PBS followed by 40 mL of 4 (w/v) % PFA. The brains were isolated and post-fixed in 4% PFA overnight and submerged in 30 (w/v) % sucrose solution for 24 hours. Tangential cortical sections of 30 μm-thickness were sliced using a cryostat and directly mounted on gelatin-subbed glass slides for immunohistological staining of GFAP (glial fibrillary acidic protein, Abcam, Cambridge, MA, USA) for astrocytes, Iba1 (ionized calcium binding adaptor molecule, Abcam, Cambridge, MA, USA) for microglial cells, Glut-1 (Glucose Transporter-1, Abcam, Cambridge, MA, USA) for endothelial cells, NF200 (Neurofilament 200, Abcam, Cambridge, MA, USA) for axonal processes, DCX (doublecortin, Abcam, Cambridge, MA, USA) for NPCs, Ki67 (Abcam, Cambridge, MA, USA) for proliferating cells, and DAPI (1:500 Invitrogen) for nuclei. Primary antibodies (1:100) were incubated overnight at 4°C and secondary antibodies (1:1000) were incubated at room temperature for two hours. A Nikon C2 confocal microscope was used to take fluorescent images.

Image analysis

Analyses were performed on microscope images of 3 coronal brain levels at +0.80 mm, -0.80 mm and -1.20 mm according to bregma, which consistently contained the cortical infarct area. Each image represents a maximum intensity projection of 10 to 12 Z-stacks, 1 um apart, captured at a 20× magnification with a Nikon C2 confocal microscope using the NIS Element software.

The endothelial (Glut-1), astrocytic (GFAP) and inflammation (Iba-1) positive area in the infarct and peri-infarct areas were quantified in 4 to 8 randomly chosen regions of interest (ROI of 0.3 mm^2). In each ROI, the positive area was measured using pixel threshold on 8-bit converted images using ImageJ (Image J v1.43, Bethesda, Maryland, USA) and expressed as the area fraction of positive signal per ROI (%). Values were then averaged across all ROI and sections, and expressed as the average positive area per animal.

The thickness of scar was measured on the ischemic boundary zone within the ipsilateral hemisphere on 3 sections stained for GFAP. The proliferating NPC cell count and migrating distance were measured on the ipsilateral hemisphere and represents the total number of doubele labeled Dcx/Ki67 positive cells present on the ventricle wall and migrating toward the infarcted zone, the maximum migration distance of NPCs was measured between the upper corner of the ipsilateral wall on the corpus callosum and the furthest Dcx/Ki67 positive cell on the migrating path toward the stroke site.

Supplementary Material

Refer to Web version on PubMed Central for supplementary material.

References

1. Go AS, Mozaffarian D, Roger VL, Benjamin EJ, Berry JD, Blaha MJ, Dai S, Ford ES, Fox CS, Franco S, Fullerton HJ, Gillespie C, Hailpern SM, Heit JA, Howard VJ, Huffman MD, Judd SE, Kissela BM, Kittner SJ, Lackland DT, Lichtman JH, Lisabeth LD, Mackey RH, Magid DJ, Marcus GM, Marelli A, Matchar DB, McGuire DK, Mohler ER 3rd, Moy CS, Mussolino ME, Neumar RW, Nichol G, Pandey DK, Paynter NP, Reeves MJ, Sorlie PD, Stein J, Towfighi A, Turan TN, Virani SS, Wong ND, Woo D, Turner MB. C American Heart Association Statistics, S Stroke Statistics. Circulation. 2014; 129:e28. [PubMed: 24352519]

2. Dibajnia P, Morshead CM. Acta Pharmacol Sin. 2013; 34:78. [PubMed: 23064725]

3. Donnan GA, Fisher M, Macleod M, Davis SM. Lancet. 2008; 371:1612. [PubMed: 18468545]

4. Kim FG, Smith JT, Reeves EE, Navalkele MJ, Grotta DD, Grau-Sepulveda JC, Hernandez MV, Peterson AF, Schwamm ED, Saver JL. Circulation. 2016

5. Taylor TN, Davis PH, Torner JC, Holmes J, Meyer JW, Jacobson MF. Stroke. 1996; 27:1459. [PubMed: 8784113] Broderick JP. Stroke. 2004; 35:205. [PubMed: 14671248]

6. Moshayedi P, Nih LR, Llorente IL, Berg AR, Cinkornpumin J, Lowry WE, Segura T, Carmichael ST. Biomaterials. 2016; 105:145. [PubMed: 27521617]

7. Reynolds BA, Weiss S. Science. 1992; 255:1707. [PubMed: 1553558] Reynolds BA, Weiss S. Dev Biol. 1996; 175:1. [PubMed: 8608856]

8. Zhang R, Zhang Z, Wang L, Wang Y, Gousev A, Zhang L, Ho KL, Morshead C, Chopp M. J Cereb Blood Flow Metab. 2004; 24:441. [PubMed: 15087713] Zhang RL, Le Tourneau Y, Gregg SR, Wang Y, Toh Y, Robin AM, Zhang ZG, Chopp M. J Neurosci. 2007; 27:3157. [PubMed: 17376977]

9. Lindvall O, Kokaia Z. Csh Perspect Biol. 2015; 7

10. Ohab JJ, Fleming S, Blesch A, Carmichael ST. J Neurosci. 2006; 26:13007. [PubMed: 17167090] Dadwal P, Mahmud N, Sinai L, Azimi A, Fatt M, Wondisford FE, Miller FD, Morshead CM. Stem Cell Reports. 2015; 5:166. [PubMed: 26235894]

11. Michalski D, Hartig W, Krueger M, Hobohm C, Kas JA, Fuhs T. Neuroreport. 2015; 26:583. [PubMed: 26053700]

12. Cook DJ, Nguyen C, Chun HN, I LL, Chiu AS, Machnicki M, Zarembinski TI, Carmichael ST. J Cereb Blood Flow Metab. 2016

13. Carmichael ST. Annals Neurol. 2016 In press.

14. Tuladhar A, Morshead CM, Shoichet MS. J Control Release. 2015; 215:1. [PubMed: 26226344] Bacigaluppi M, Russo GL, Peruzzotti-Jametti L, Rossi S, Sandrone S, Butti E, De Ceglia R, Bergamaschi A, Motta C, Gallizioli M. Journal of Neuroscience. 2016; 36:10529. [PubMed: 27733606]

15. Moshayedi P, Carmichael ST. Biomatter. 2013; 3

16. Fraser JR, Laurent TC, Pertoft H, Baxter E. Biochem J. 1981; 200:415. [PubMed: 7340841]

17. Lam J, Lowry WE, Carmichael ST, Segura T. Adv Funct Mater. 2014; 24:7053. [PubMed: 26213530]

18. Zhu S, Nih L, Carmichael ST, Lu Y, Segura T. Adv Mater. 2015; 27:3620. [PubMed: 25962336]

19. Griffin DR, Weaver WM, Scumpia PO, Di Carlo D, Segura T. Nat Mater. 2015; 14:737. [PubMed: 26030305]

20. Sideris E, Griffin DR, Ding Y, Li S, Weaver WM, Di Carlo D, Hsiai T, Segura T. ACS Biomaterials Science & Engineering. 2016

21. Carmichael ST. NeuroRx. 2005; 2:396. [PubMed: 16389304]

22. Madden LR, Mortisen DJ, Sussman EM, Dupras SK, Fugate JA, Cuy JL, Hauch KD, Laflamme MA, Murry CE, Ratner BD. Proceedings of the National Academy of Sciences. 2010; 107:15211.Sokic S, Christenson M, Larson J, Papavasiliou G. Macromolecular bioscience. 2014; 14:731. [PubMed: 24443002] Stachowiak AN, Bershteyn A, Tzatzalos E, Irvine DJ. Advanced Materials. 2005; 17:399.

23. Inta D, Cameron HA, Gass P. Trends Neurosci. 2015; 38:517. [PubMed: 26298770]

24. Tokatlian T, Cam C, Siegman SN, Lei Y, Segura T. Acta biomaterialia. 2012; 8:3921. [PubMed: 22820309]

25. Nih LR, Deroide N, Lere-Dean C, Lerouet D, Soustrat M, Levy BI, Silvestre JS, Merkulova-Rainon T, Pocard M, Margaill I, Kubis N. Eur J Neurosci. 2012; 35:1208. [PubMed: 22512253]

26. Berdichevski A, Simaan Yameen H, Dafni H, Neeman M, Seliktar D. Proc Natl Acad Sci U S A. 2015; 112:5147. [PubMed: 25825771]
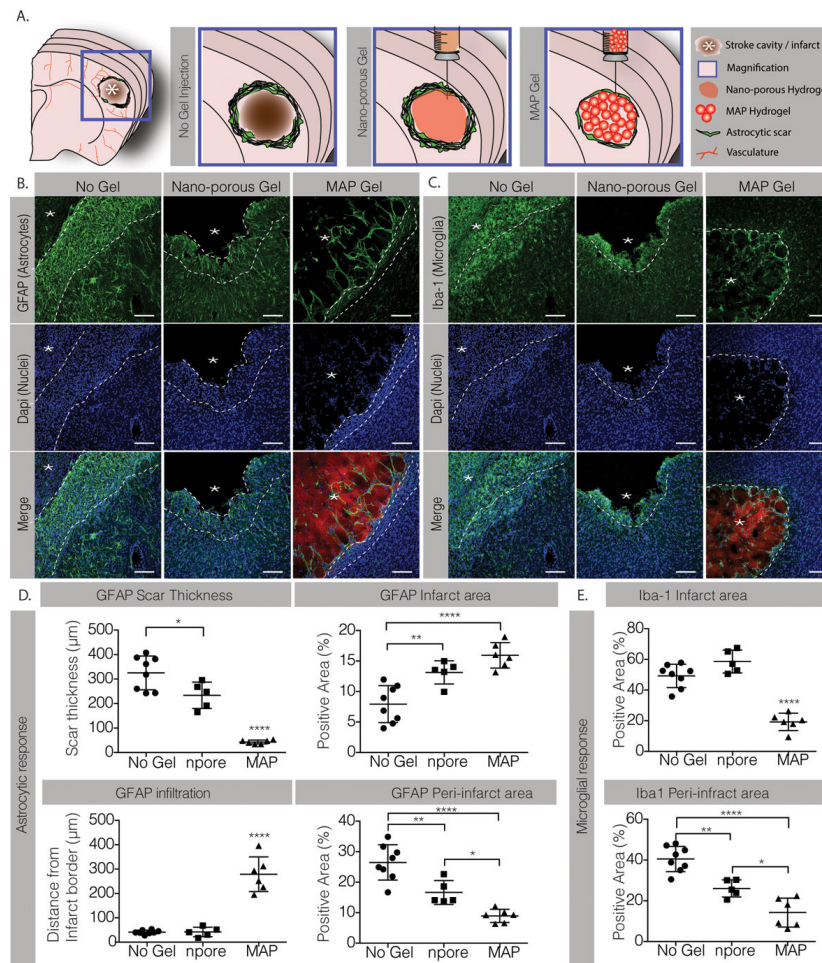
Figure 1.
A. Schematic illustration of a coronal mouse brain section showing the location of the cortical stroke cavity. The magnified schematics illustrate the no gel, the nano-porous and the MAP hydrogel injection conditions. B. Fluorescent images of GFAP staining showing post-stroke astrocytic response in the different conditions (scale 100 μm). C. Iba-1 staining showing post-stroke microglial response in the different conditions (scale 100 μm). D. Analysis of the GFAP positive response in terms of scar thickness, astrocytic infiltration in the infarct area and the positive area for GFAP signal in both infarct and peri-infarct regions. E. Analysis of the Iba-1 positive response in terms of positive area for GFAP signal in both infarct and peri-infarct regions. *, ** and **** indicate P < 0.05, P < 0.01 and P < 0.0001, respectively (Anova 1 way, Tukey's opst-hoc test).
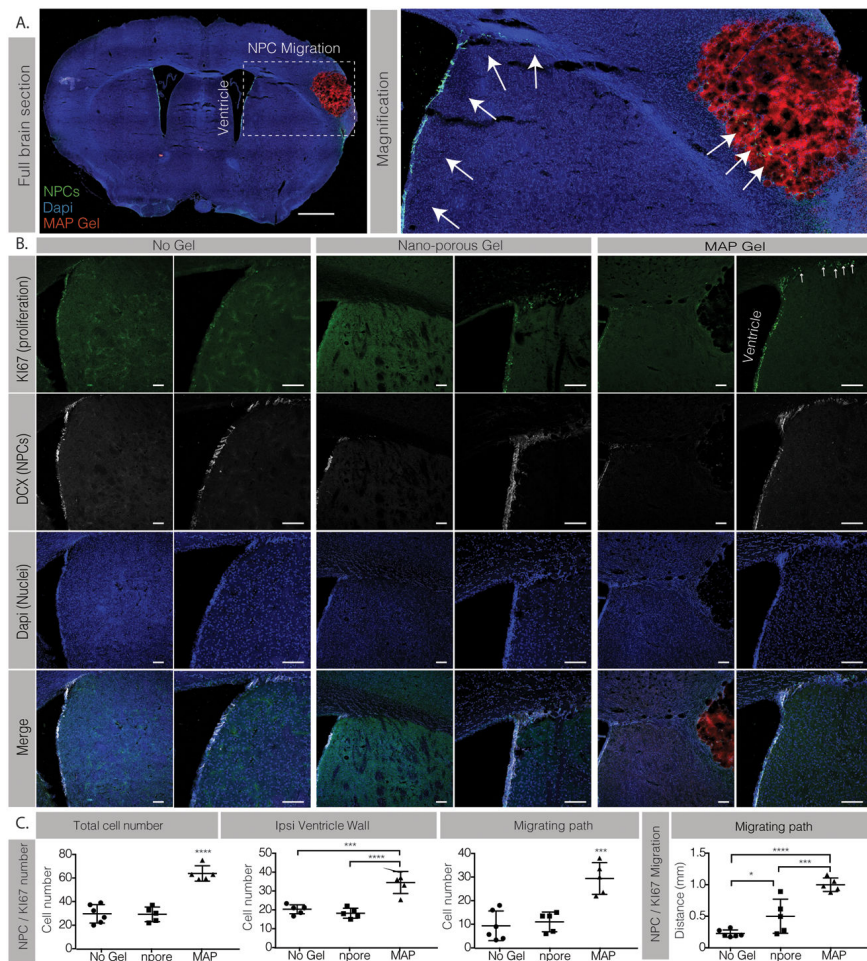
Figure 2.
A. Full section fluorescent image and magnification showing DCX positively labeled NPCs (green) migrating from the ipsilateral ventricle to the stroke area (scale 0.5mm). B. Co-staining of Ki67 (green) and DCX positive NPCs (white) (scale 100μm). C. Analysis of KI67 / DCX total cell number and migrating distance. *, *** and **** indicate P < 0.05, P < 0.001 and P < 0.0001, respectively (Anova 1 way, Tukey's opst-hoc test).
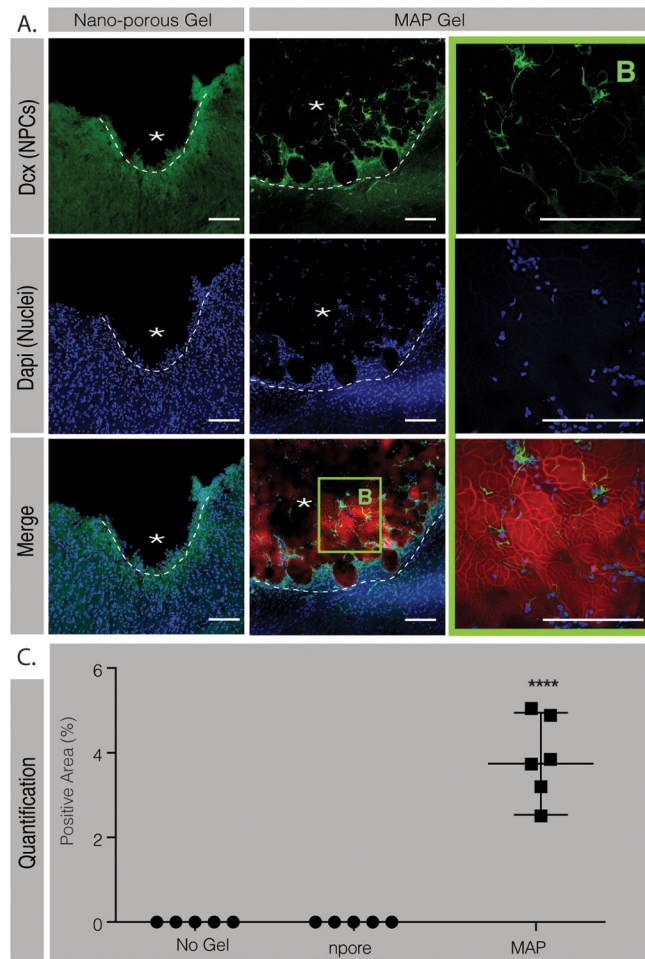
Figure 3.
A. Fluorescent images and B. magnification of the stroke area in both the nanoporous and the MAP gel condition showing DCX positive cells (green) in the lesion site of the MAP–treated animals only (scale 100 μm). C. Analysis of the positive area for DCX signal in the stroke site in the different conditions. **** indicates P < 0.0001 (Anova 1 way, Tukey's opst-hoc test).

Injection of Microporous Annealing Particle (MAP) Hydrogels in the Stroke Cavity Reduces Gliosis and Inflammation and Promotes NPC Migration to the Lesion
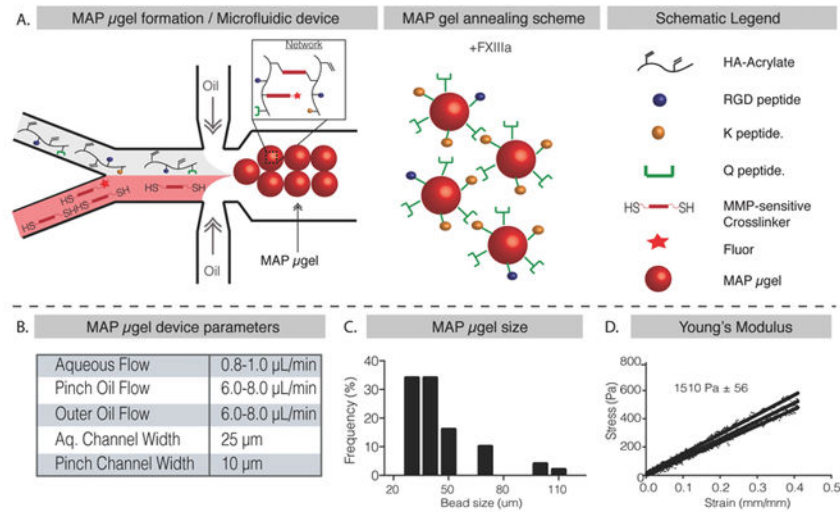
Scheme 1.
A. Schematic illustration of flow focusing microfluidic device to produce μgels that can be annealed to each other using enzyme factor XIII to form a scaffold. B. Important flow rates and device parameters to produce the μgels. C. Distribution of μgels diameters produced using the microfluidic device. D. Young's Modulus in compression calculated using Instron mechanical tests showing scaffold stiffness similar to brain cortex